

# Microstructure and properties of Mg–Zn ferrite as a result of sintering temperature

Zbigniew Pędzich<sup>a,\*</sup>, Mirosław M. Bućko<sup>a</sup>, Michał Królikowski<sup>a</sup>,  
Małgorzata Bakalarska<sup>b</sup>, Joanna Babiarsz<sup>b</sup>

<sup>a</sup>University of Mining and Metallurgy, Faculty of Materials Science and Ceramics, al. Mickiewicza 30, 30-059 Cracow, Poland

<sup>b</sup>LG.Philips Displays Poland, ul. Zwierzyniecka 2, 96-100 Skierniewice, Poland

## Abstract

This paper presents results of investigations on property changes of Mg–Zn ferrite used commercially for deflection yoke cores sintered at temperatures ranging from 900 to 1400 °C. Physical and mechanical properties were determined: apparent density, strength, elastic properties. The most important magnetic properties as initial permeability, coercivity, saturation magnetic flux, retentivity and Curie point temperature were determined. Microstructure evolution during sintering was observed and compared with changes of mechanical and magnetic properties as well as electrical conductivity. Presented results could be helpful in optimisation of ferrite heat-treatment conditions.

© 2003 Elsevier Ltd. All rights reserved.

**Keywords:** Ferrites

## 1. Introduction

From the early days of ferrites commercial application as a TV deflection yoke Mn–Zn ferrites were the material of choice. These materials connected good magnetic properties with low production costs. Introduction of High Definition Television (HDTV) changed the situation. Significant increase in horizontal grids meant that ferrite material had to be effective at a higher frequency. It means that ferrite used in HDTV application should have higher resistivity than the Mn–Zn one ( $\sim 10^2 \Omega\cdot\text{cm}$ ).<sup>1</sup> Mentioned problem could be solved with the utilization of Mg–Zn ferrite. Although, the most of magnetic parameters are better for Mn–Zn ferrites, the decisive parameter is resistivity much higher for Mg–Zn materials ( $\sim 10^6\text{--}10^7 \Omega\cdot\text{cm}$ ). Processing of Mg–Zn ferrites should be provided with care on their densification, microstructure and mechanical properties to assure possible high values of magnetic properties.

The present work shows the results of investigation on influence of sintering conditions of commercially utilised Mg–Zn ferrite powder on product properties.

The aim of the research was to optimise manufacturing of ferrite with suitable magnetic properties accompanied with as good as possible mechanical properties.

## 2. Experimental

All investigation, conducted in the presented work, based on commercially utilized by LG.Philips Displays Poland Mg–Zn ferrite powder (containing a small amount of Mn). This powder mixed with plastifiers was uniaxial pressed under 50 MPa. Samples in O-ring shape were sintered in a furnace with Superkanthal 1900 heating elements in air atmosphere. The maximum sintering temperature ranged from 900 to 1400 °C with 100 °C steps. The heating rate was 10 °C/min. The soaking time at maximum temperature was 2 h in each case.

Apparent density ( $\rho$ ) and water wettability ( $W$ ) of sintered samples were determined by the Archimedian method. The strength of sintered bodies was estimated by diagonal compression tests of O-rings. The destructive compression stresses ( $\sigma_u$ ) were calculated utilizing Frocht's formulas:<sup>2</sup>

$$\sigma_u = P \cdot K / (D - 2d) \cdot h$$

\* Corresponding author. Tel.: + 48-12617-2397; fax: +48-12633-4630.

E-mail address: [pedzich@uci.agh.edu.pl](mailto:pedzich@uci.agh.edu.pl) (Z. Pędzich).

Table 1

Results of densification parameters ( $\rho$ ,  $W$ ), ultrasonic wave propagation velocity measurements ( $v_L$ ,  $v_T$ ), strength estimation of O-ring samples ( $\sigma_u$ ) and grain size changes ( $M$ ,  $\sigma_M$ ) for all sintered samples

Sintering conditions	Apparent density ( $\rho$ , g/cm <sup>3</sup> )	Wetability, $W$ (%)	Longitudinal ultrasonic wave velocity, $v_L$ (m/s)	Transverse ultrasonic wave velocity, $v_T$ (m/s)	Destructive compressive stress, $\sigma_u$ (MPa)	Mean grain size, $M$ ( $\mu$ m)	Mean grain size deviation, $\sigma_M$ ( $\mu$ m)
Starting powder	—	—	—	—	—	0.5	—
900 °C	2.57 $\pm$ 0.2 <sup>a</sup>	17.2 $\pm$ 0.3	2260.8 $\pm$ 19.7	1344.2 $\pm$ 37.8	0.75 $\pm$ 0.07	0.5	0.2–1.0 <sup>b</sup>
1000 °C	3.10 $\pm$ 0.2	10.5 $\pm$ 0.3	3885.4 $\pm$ 18.0	2375.7 $\pm$ 30.8	3.18 $\pm$ 0.46	1.0	0.5–2.5 <sup>b</sup>
1100 °C	4.07 $\pm$ 0.2	2.7 $\pm$ 0.3	6297.6 $\pm$ 42.3	3572.7 $\pm$ 10.5	9.48 $\pm$ 0.82	1.4	0.6
1200 °C	4.46 $\pm$ 0.1	0	7127.8 $\pm$ 115.6	3864.8 $\pm$ 32.5	12.08 $\pm$ 2.10	4.1	2.1
1300 °C	4.46 $\pm$ 0.1	0	7181.9 $\pm$ 112.9	3882.0 $\pm$ 20.2	10.94 $\pm$ 1.31	10.6	5.5
1400 °C	4.48 $\pm$ 0.1	0	7250.2 $\pm$ 92.6	3914.8 $\pm$ 25.9	6.79 $\pm$ 0.39	16.9	8.3

<sup>a</sup>  $\pm$ , denotes standard deviation of mean value.

<sup>b</sup> Denotes range of grain size distribution.

where:  $P$  is a load at destruction moment;  $K$  the coefficient of stress concentration (assumed in our calculations as (1);  $D$ ,  $d$  and  $h$  are the external diameter, internal diameter and height of the ring, respectively. Tests were performed using ZWICK 1435 apparatus.

The microstructural analyses of sintered bodies encompass SEM (Philips XL30) and optical microscopy (Nikon Ehipot 300) observations of polished sample surfaces after chemical etching. The microstructural parameters as a mean grain size ( $M$ ) and mean grain size deviation ( $\sigma_M$ ) were determined by Saltykov's method.<sup>3</sup>

The X-ray diffraction patterns analysis (Seifert XRD7) was helpful in phase identification and calculation of unit cell parameter values for ferrite powder and sintered materials.

Electrical conductivity of samples was measured using Hewlett Packard HP33501A multimeter at temperatures ranged from 200 to 700 °C.

Longitudinal ( $v_L$ ) and transverse ( $v_T$ ) ultrasonic waves propagation velocity measurements were performed with INCO (Poland) equipment.

The basic magnetic parameters as Curie temperature ( $T_C$ ), initial permeability ( $\mu_i$ ), coercivity ( $H_c$ ), saturation magnetic flux ( $B_{sat}$ ) and retentivity ( $B_r$ ) were determined using dynamic methods.

### 3. Results

Table 1 summarized densification parameters ( $\rho$ ,  $W$ ), ultrasonic wave propagation velocity measurements results ( $v_L$ ,  $v_T$ ), strength estimation of O-ring samples ( $\sigma_u$ ) and grain size parameters ( $M$ ,  $\sigma_M$ ) for all sintered bodies. Samples sintered at temperatures ranging from 1200 °C and higher shows no wetability. Their apparent density is practically stable. In samples sintered at lower temperatures significant porosity can strongly influence measured properties (mechanical, elastic and magnetic).

Strength of the samples estimated by destructive compressive stress  $S$  is low for these with open porosity. Maximum strength is reached for dense ferrite body with the smallest grain size. Increase of heat treatment temperature causes significant grain growth and strength decrease.

Ultrasonic measurements show that for samples with stable, high density wave propagation velocity slightly increases with grain size increase. It means that grain boundaries influence ultrasonic wave propagation. In the material with small grains (i.e. a large amount of boundaries) ultrasonic waves propagate slower than in ferrites with big grains. It suggests that grain boundaries are probably not homogenous.

Fig. 1 demonstrates an X-ray diffraction pattern achieved for a sample sintered at 1300 °C. Such an image is typical for all investigated samples. Only one non-stoichiometric phase with Fd3m structure (corresponding to franklinite type for the Zn–Fe–O system<sup>4</sup>) could be detected in each pattern. Fig. 2 illustrates changes of unit cell parameter  $a$  due to sintering temperature. Up to sintering temperature of 1100 °C parameter  $a$  has the same value, above this temperature significant increase of  $a$  value is observed. These

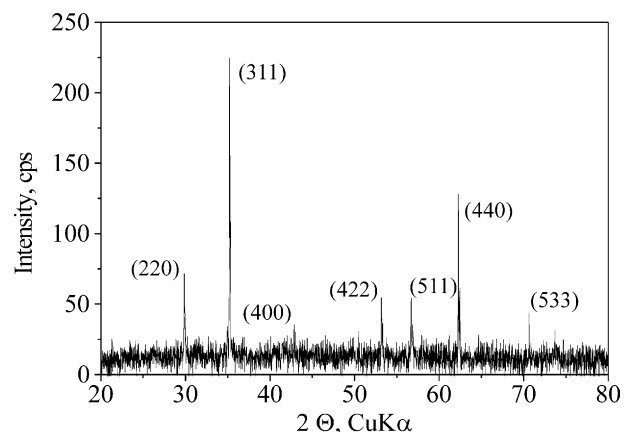


Fig. 1. The X-ray diffraction pattern of the sample sintered at 1300 °C.

changes are the most probably due to the various occupation of cation positions in the spinel structure. The iron and manganese cations valency changes ( $\text{Fe}^{+2} \leftrightarrow \text{Fe}^{+3}$  and  $\text{Mn}^{+2} \leftrightarrow \text{Mn}^{+3}$ ) may cause the cations to occupy different Wyckoff positions according to their charge,  $a$  and  $d$  respectively.<sup>5</sup>

Description of microstructure evolution could be completed with data included in Fig. 3, where the cumulative curves of grain size distribution for materials sintered at 1100–1400 °C were plotted. These data show that in samples sintered at 1300 and 1400 °C an exaggerated grain growth occurred. Microstructures of the mentioned ferrites are given in Fig. 4.

The basic magnetic property values are collected in Table 2. The most suitable properties show materials sintered at 1200 and 1300 °C. They have the highest values of initial permeability, saturation magnetic flux and retentivity. The coercivity of these materials is the lowest among investigated materials.

The measurement of electrical resistance as a function of temperature allows us to calculate conductivity of the

investigated material. The data plotted in Arrhenius' coordinates make it possible to estimate activation energy of ferrite conductivity. Fig. 5 compares results of measurements for materials sintered at 1100 and 1400 °C. Coefficients  $a_{ii}$  placed in the figure are slopes of estimation lines correlated with activation energy of conductivity. Both calculated curves have two ranges of linearity (200–440 °C and 440–700 °C). At higher temperatures, where the structure decides on conductivity, values of activation energy are similar. It suggests that the structure of the grain interiors are almost the same in both ferrites. At lower temperatures some additional factors such as: distribution of respective cations, concentration of impurities or/and differences in microstructure influence the conductivity. Conductivity plots compared in Fig. 5 concern two relatively dense ferrites with significantly different microstructure (grain size and amount of grain boundaries) and unit cell parameters. Generally, the electrical resistance measurements show that materials sintered at higher temperatures have lower resistance.

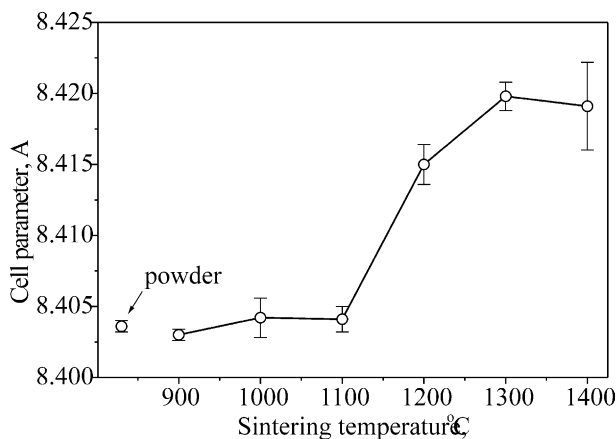


Fig. 2. The unit cell parameter  $a$  changes vs sintering temperature.

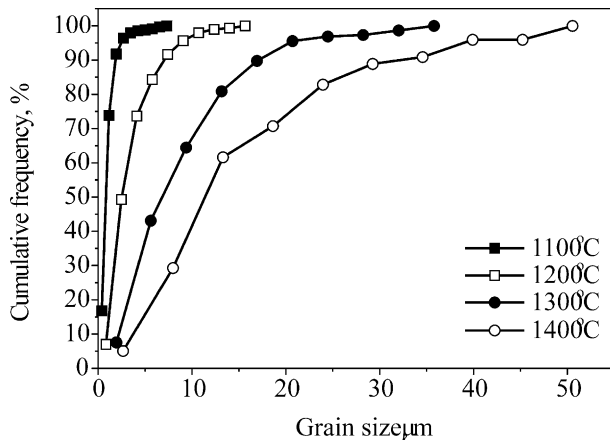
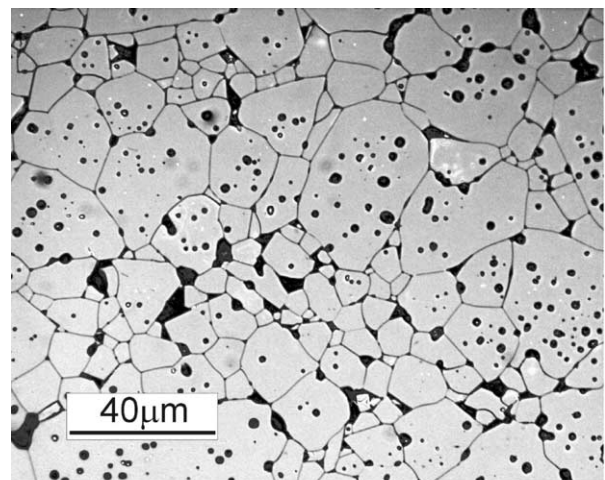
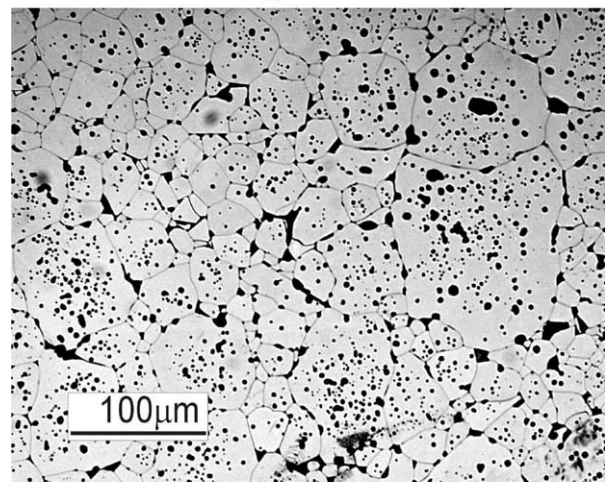


Fig. 3. Cumulative curves of grain size distribution in ferrites sintered at indicated temperatures.



(a)



(b)

Fig. 4. Microstructures of polished and etched surfaces of ferrite bodies sintered at 1300 (a) and 1400 °C (b).

Table 2  
Basic magnetic properties of investigated samples

Sintering conditions	Initial permeability, $\mu_i$ , (mT)	Coercivity, $H_c$ , (Am)	Saturation magnetic flux, $B_{sat}$ , (mT)	Retentivity, $B_r$ , (mT)	Curie temperature, $T_C$ (°C)
900 °C	13	—	25	6.3	136
1000 °C	43	252	88	59	141
1100 °C	215	104	203	163	141
1200 °C	467	36	234	175	142
1300 °C	569	23	248	173	145
1400 °C	549	21	246	148	151

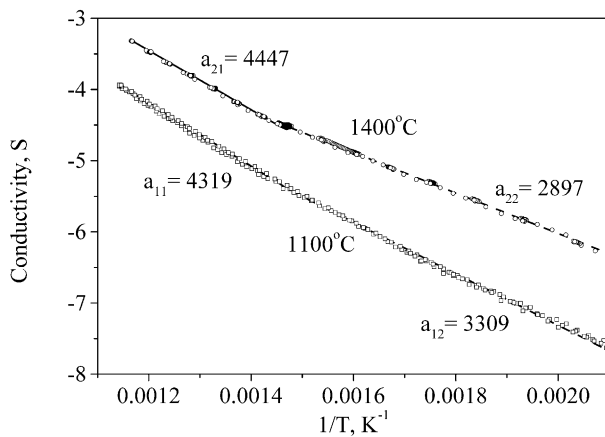


Fig. 5. Arrhenius' plot of conductivity of ferrites sintered at indicated temperatures. The  $a_{ij}$  parameters are the measure of activation energy of conductivity at different temperature ranges.

#### 4. Summary

A concise characteristic of different ferrite properties as a function of sintering temperature given above shows that definition of the optimal method of ferrite heat-treatment requires the reconciling of opposing tendencies in temperature dependence of individual properties.

Maximisation of magnetic parameter values demands high sintering temperature (1300 °C). However, such heat-treatment conditions cause an exaggerated grain growth and significantly a decrease of mechanical strength.

The measurements of ultrasonic wave propagation velocity indicate that the grain growth is accompanied with wave propagation velocity increase. Because the densities of samples sintered at 1200–1400 °C are practically the same, mentioned increase could be ascribed to microstructure changes—amount of grain boundaries decrease and probably more uniform distribution of impurities. It is confirmed by the decrease of ferrite resistivity with sintering temperature increase. This fact can be attributed to lower amount of grain boundaries.

#### References

1. Goldman, A., *Handbook of Modern Ferromagnetic Materials*. Kluwer Academic Publishers, Boston-Dordrecht-London, 1999.
2. Frocht, M. M., *Photoelasticity*. Wiley, New York, 1949.
3. Saltykov, S., *Stereometric Metallurgy*. Metallurgia Publ., Moscow, 1950.
4. JCPD-ICDD card No. 22-1012.
5. Lucchesi, S., Russo, U. and Della Giusta, A., Crystal chemistry and cation distribution in some Mn-rich natural and synthetic spinels. *European Journal of Mineralogy*, 1997, **9**, 31–42.